J|A|C|S
ARTICLES
Published on Web 12/10/2002

Internal Degrees of Freedom, Structural Motifs, and Conformational Energetics of the 5′-Deoxyadenosyl Radical: Implications for Function in Adenosylcobalamin-Dependent Enzymes. A Computational Study

Dmitry V. Khoroshun, Kurt Warncke, Shyue-Chu Ke, Djamaladdin G. Musaev, and Keiji Morokuma*

Contribution from the Cherry L. Emerson Center for Scientific Computation, Department of Chemistry and Department of Physics, Emory University, Atlanta, Georgia 30322, and Department of Physics, National Dong Hwa University, Taiwan

Received September 3, 2002; E-mail: morokuma@emory.edu

Abstract: The potential energy surface of the free 5′-deoxyadenosyl radical in the gas phase is explored using density functional and second-order Møller−Plesset perturbation theories with 6-31G(d) and 6-31++G-(d,p) basis sets and interpreted in terms of attractive and repulsive interactions. The 5′,8-cyclization is found to be exothermic by ∼20 kcal/mol but kinetically unfavorable; the lowest cyclization transition state (TS) lies about 7 kcal/mol higher than the highest TS for conversion between most of the open isomers. In open isomers, the two energetically most important attractive interactions are the hydrogen bonds (a) between the 2′-OH group and the N3 adenine center and (b) between the 2′-OH and 3′-OH groups. The relative ribose−adenine rotation about the C1′−N9 glycosyl bond in a certain range changes the energy by as much as 10−15 kcal/mol, the origin being (i) the repulsive 2′-H···H−C8 and O1′···N3 and (ii) the attractive 2′-OH···N3 ribose−adenine interactions. The hypothetical synergy between the glycosyl rotation and the Co−C bond scission may contribute to the experimentally established labilization of the Co−C bond in enzyme-bound adenosylcobalamin. The computational results are not inconsistent with the rotation about the C1′−N9 glycosyl bond being the principal coordinate for long-range radical migration in coenzyme B_{12}-dependent enzymes. The effect of the protein environment on the model system results reported here remains an open question.

1. Introduction

The 5′-deoxyadenosyl radical, $AdCH_2^•$ (Scheme 1), initiates the radical rearrangement reactions that are catalyzed by the members of the adenosylcobalamin-dependent and *S*-adenosylmethionine-dependent enzyme families.[1] In the enzymes dependent on *S*-adenosylmethionine (AdoMet), $AdCH_2^•$ is formed by cleavage of the S−C5′ bond. In the enzymes of the adenosylcobalamin (AdoCbl; coenzyme B_{12}) family, $AdCH_2^•$ is formed by cleavage of the Co−C5′ bond. Despite its proposed central role in hydrogen atom abstraction and radical-mediated catalysis in AdoMet- and AdoCbl-dependent enzymes,[1] $AdCH_2^•$ has not been observed directly in experiment. Therefore, we chose to study computationally the free, gas-phase $AdCH_2^•$ as the first step toward understanding the role of the $AdCH_2^•$ moiety in enzyme catalysis.

The 5′-deoxyadenosyl moiety is involved in three steps of a mechanism for radical-mediated catalysis in the adenosylcobalamin-dependent enzymes, as depicted in Scheme 2.[2] First, $AdCH_2^•$ is released into the active site following the Co−C bond cleavage at stage a. Second, at stage b, $AdCH_2^•$ undergoes a deformation, with the C5′ center being displaced by as much as 5−7 Å relative to the Co(II) center. Third, the 5′-deoxy-

Scheme 1. Atomic Notation and the Descriptors of Internal Degrees of Freedom for the 5′-Deoxyadenosyl Radical[a]

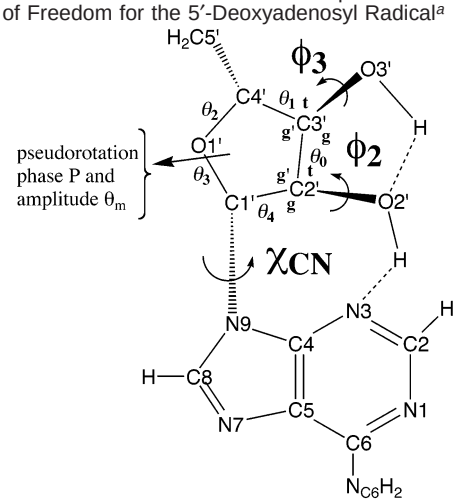

[a] The exocyclic ribose dihedral angles: (ϕ_2) C1′−C2′−O2′−O2′H, (ϕ_3) C2′−C3′−O3′−O3′H, (χ_{CN}) O1′−C1′−N9−C8. The endocyclic ribose dihedral angles (θ_0) C1′−C2′−C3′−C4′, (θ_1) C2′−C3′−C4′−O1′, (θ_2) C3′−C4′−O1′−C1′, (θ_3) C4′−O1′−C1′−C2′, (θ_4) O1′−C1′−C2′−C3′ are described by the pseudorotation phase, *P*, and amplitude, θ_m, as described in eq 3.

(1) (a) Frey, P. A. *Ann. Rev. Biochem.* **2001**, *70*, 121. (b) *Chemistry and Biochemistry of B_{12}*; Banerjee, R., Ed.; Wiley: New York, 1999. (c) Marsh, E. N. G.; Drennan, C. L. *Curr. Opin. Chem. Biol.* **2001**, *5*, 499.
(2) Booker, S.; Licht, S.; Broderick, J.; Stubbe, J. *Biochemistry* **1994**, *33*, 12676.

10.1021/ja028393k CCC: $25.00

Scheme 2. Minimal Mechanism for Coenzyme B_{12}-Dependent Enzyme Catalysis, Showing Pathways of Radical Migration in Vitamin B_{12} Coenzyme-Dependent Enzymes[1] [a]

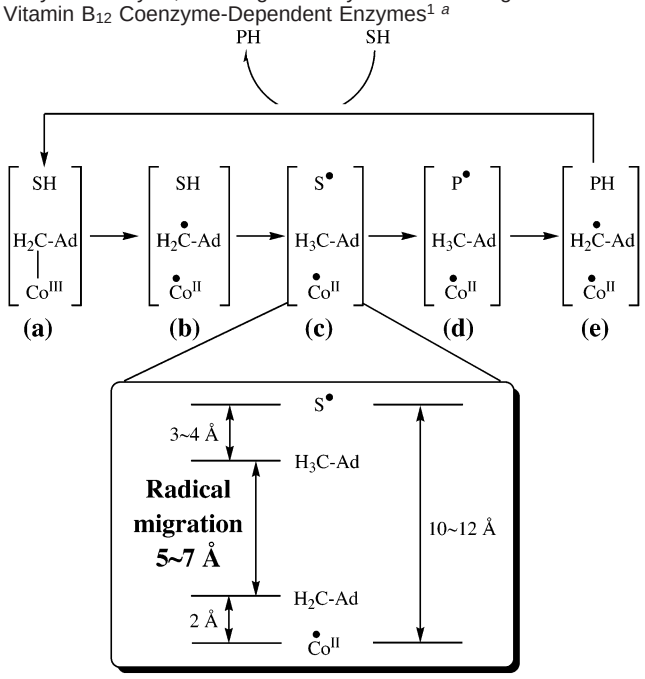

[a] Additional intermediates and reactions are present in the mechanism of the net redox reaction catalyzed by coenzyme B_{12}-dependent ribonucleotide reductase.[2,6] The forward direction of reaction is indicated by arrows. Substrate-derived species in the radical pair states are designated SH (bound substrate), S• (substrate radical), P• (product radical), and PH (bound product). The 5′-deoxyadenosyl moiety is represented as Ad−CH_2− (AdoCbl β-axial ligand) in the intact coenzyme and as Ad−CH_2• (5′-deoxyadenosyl radical) or Ad−CH_3 (5′-deoxyadenosine) following cobalt−carbon bond cleavage. Outlined is the summary of the relevant experimental data[3,5,7−10] on Class II enzymes such as ethanolamine deaminase; the deoxyadenosyl moiety is depicted twice, symbolizing the location of the C5′ center at stage a as Ad−CH_2 and at stage c as Ad−CH_3.

adenosyl moiety is involved in a hydrogen atom transfer with the substrate (product) of the enzymatic reaction, stages c−e of Scheme 2.

The separation between the two radical centers at stage c, the Co(II) atom and the source of the hydrogen atom for the abstraction by the C5′ center, has been experimentally measured for several coenzyme B_{12}-dependent enzymes. The Co(II)−S• radical distance in diol dehydrase, 10 Å[3] (a value of 8.4 Å is obtained for the Co(II)−S• distance in the X-ray crystallographic structure of the diamagnetic state),[4] the Co(II)−S• radical distance in ethanolamine deaminase (also known as ethanolamine-ammonia lyase), 10−12 Å,[3,5] and the Co(II)−thiyl radical distance in coenzyme B_{12}-dependent ribonucleotide triphosphate reductase, 8 Å,[6] indicate that a relatively long-range C5′ center migration is characteristic of class II enzymes. In ethanolamine deaminase,[7] the radical migration has been particularly well characterized. Electron spin−echo envelope modulation (ESEEM)[8] and electron−nuclear double resonance (ENDOR)[9] studies of ethanolamine deaminase reveal that C5′ of $AdCH_3$ in the Co(II)−S• radical pair at stage c is 3.2−3.4 Å from the substrate radical center. The Co−C distance at stage a, ∼2.0 Å,[10] is also known. Orientation−selection ESEEM studies show that the Co(II)−C5′ distance is 7.8−8.3 Å.[5] Thus, as depicted in Scheme 2, the C5′ radical center shuttles over a distance of 5−7 Å at stage b of the operating mechanism for ethanolamine deaminase. In the class I mutases, the Co center and the S/P atoms involved in hydrogen migration are separated by shorter, yet substantial, distances of approximately 6−7 Å,[11] and the C5′ migration may involve smaller displacements[12] of <3 Å. Therefore, displacements of the C5′ radical center have been established as a common theme in the functioning of adenosylcobalamin-dependent enzymes at stage b. Another prominent feature of the adenosylcobalamin-dependent enzymes is the substantial, by as much as 15 kcal/mol, decrease of the Co−C bond dissociation energy of coenzyme B_{12} within certain holoenzymes compared to that of free B_{12} in solution.[13]

Changes in several internal degrees of freedom of the 5′-deoxyadenosyl moiety have previously been discussed within the context of processes at stages a and b. The relative ribose−adenine rotation about the glycosyl C1′−N9 bond[14] and the ribose pseudorotation[12] have been suggested to mediate the C5′ movement. Binding interactions of corrin[14b] and adenine[14b,15] moieties of coenzyme B_{12} with the protein have been proposed to pull the two moieties apart from each other, weakening the Co−C5′ bond. The angular strains associated with Co−C5′−C4′ and ligand−Co−C5′ angles were also proposed by Pratt to labilize the Co−C bond.[16] Finally, the C5′ radical quenching side processes, the experimentally observed 5′,8-cyclization,[13] and the tentatively suggested 8→5′ hydrogen transfer[17] also might occur within the $AdCH_2$• moiety.

Previous extensive theoretical studies of coenzyme B_{12} and coenzyme models have focused on factors influencing the Co−C5′ bond homolysis,[18] the Co coordination sphere,[19] and pathways of substrate rearrangement.[20] At the same time, no systematic computations have been performed on the internal degrees of freedom of the 5′-deoxyadenosyl radical and its

(3) Boas, J. F.; Hicks, P. R.; Pilbrow, J. R.; Smith, T. D. *J. Chem. Soc., Faraday Trans. 2* **1978**, *74*, 417.
(4) Shibata, N.; Masuda, J.; Tobimatsu, T.; Toraya, T.; Suto, K.; Morimoto, Y.; Yasuoka, N. *Structure* **1999**, *7*, 997.
(5) Canfield, J. M.; Warncke, K. *J. Phys. Chem. B.* **2002**, *106*, 8831.
(6) (a) Buettner, G. R.; Coffman, R. E. *Biochim. Biophys. Acta* **1977**, *480*, 495. (b) Gerfen, G. J.; Licht, S.; Willems, J.-P.; Hoffman, B. M.; Stubbe, J. *J. Am. Chem. Soc.* **1996**, *118*, 8192. (c) Licht, S.; Gerfen, G. J.; Stubbe, J. *Science* **1996**, *271*, 477.
(7) (a) Babior, B. M. Ethanolamine Ammonia-Lyase. In *B_{12}*; Dolphin, D., Ed.; Wiley: New York, 1982; Vol. 2, pp 263−287. (b) Bandarian, V.; Reed, G. H. Ethanolamine Ammonia-Lyase. In *Chemistry and Biochemistry of B_{12}*; Banerjee, R., Ed.; Wiley: New York, 1999; pp 811−833.
(8) Warncke, K.; Utada, A. S. *J. Am. Chem. Soc.* **2001**, *123*, 8564.
(9) LoBrutto, R.; Bandarian, V.; Magnusson, O. T.; Chen, X.; Schramm, V. L.; Reed, G. H. *Biochemistry* **2001**, *40*, 9.
(10) Structures FIZMUW in Cambridge Structural Database: (a) Savage, H. F. J.; Lindley, P. F.; Finney, J. L.; Timmins, P. A. *Acta Crystallogr.* **1987**, *B43*, 280. (b) Allen, F. H.; Kennard, O. *Chemical Design Automation News* **1993**, *8*, 1.
(11) (a) Bothe, H.; Darley, D. J.; Albracht, S. P. J.; Gerfen, G. J.; Golding, B. T.; Buckel, W. *Biochemistry* **1998**, *37*, 4105. (b) Mancia, F.; Smith, G. A.; Evans, P. R. *Biochemistry* **1999**, *38*, 7999. (c) Mancia, F.; Keep, N. H.; Nakagawa, A.; Leadlay, P. F.; McSweeney, S.; Rasmussen, B.; Boesecke, P.; Diat, O.; Evans, P. R. *Structure* **1996**, *4*, 339. (d) Mancia, F.; Evans, P. R. *Structure* **1998**, *6*, 711. (e) Reitzer, R.; Grueber, K.; Jogl, G.; Wagner, U. G.; Bothe, H.; Buckel, W.; Kratky, C. *Structure* **1999**, *7*, 891. (f) Gerfen, G. J. In *Chemistry and Biochemistry of B_{12}*; Banerjee, R., Ed.; Wiley: New York, 1999; pp 165−195.
(12) Gruber, K.; Reitzer, R.; Kratky, C. *Angew. Chem., Int. Ed.* **2001**, *40*, 3377.
(13) (a) Finke, R. G.; Hay, B. P. *Inorg. Chem.* **1984**, *23*, 3041. (b) Hay, B. P.; Finke, R. G. *J. Am. Chem. Soc.* **1987**, *109*, 8012. (c) Garr, C. D.; Sirovatka, J. M.; Finke, R. G. *J. Am. Chem. Soc.* **1996**, *118*, 11142.
(14) (a) Pett, V. B.; Liebman, M. N.; Murray-Rust, P.; Prasad, K.; Glusker, J. P. *J. Am. Chem. Soc.* **1987**, *109*, 3207. (b) Masuda, J.; Shibata, N.; Morimoto, Y.; Toraya, T.; Yasuoka, N. *Structure* **2000**, *8*, 775.
(15) (a) Toraya, T.; Matsumoto, T.; Ichikawa, M.; Itoh, T.; Sugawara, T.; Mizuno, Y. *J. Biol. Chem.* **1986**, *261*, 9289. (b) Toraya, T.; Watanabe, N.; Ichikawa, M.; Matsumoto, T.; Ushio, K.; Fukui, S. *J. Biol. Chem.* **1987**, *262*, 8544.
(16) (a) Pratt, J. M. In *B_{12}*; Dolphin, D., Ed.; Wiley: New York, 1982; Vol. 1, pp 325−392. (b) Pratt, J. M. *J. Mol. Catal.* **1984**, *23*, 187. (c) Pratt, J. M. *Chem. Soc. Rev.* **1985**, *14*, 161.
(17) Sando, G. N.; Blakley, R. L.; Hogenkamp, H. P. C.; Hoffmann, P. J. *J. Biol. Chem.* **1975**, *250*, 8774.

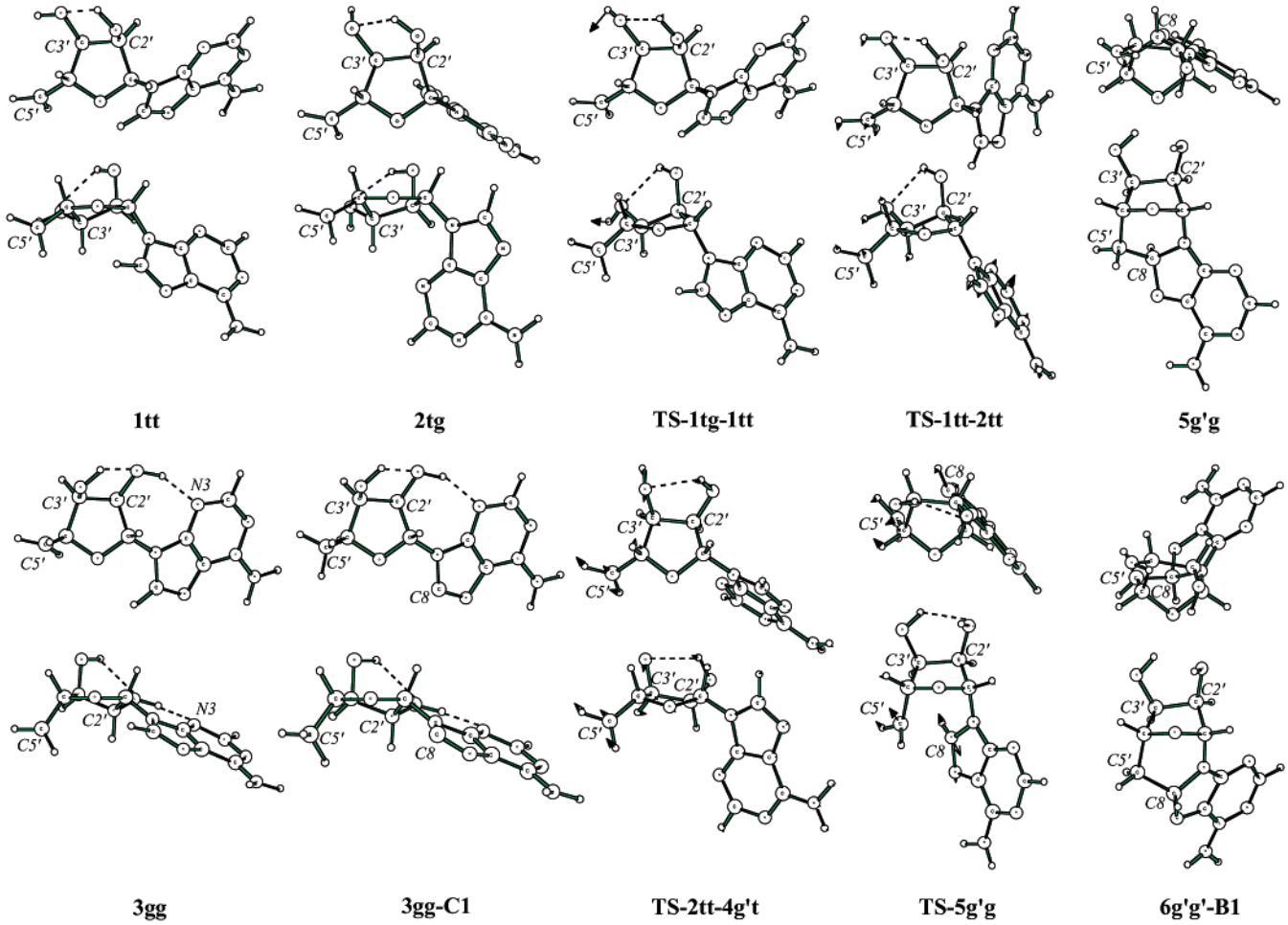

Figure 1. Structures of selected stationary points. The reaction coordinates for the transition states are depicted by arrows at atoms.

potential roles in coenzyme B_{12}-dependent catalysis. We have therefore focused on the free 5′-deoxyadenosyl radical in the present computational study.

2. Theoretical Methods

The present study explores the potential energy surface (PES) of a substantially large (18 non-hydrogen atoms), floppy molecule using the stationary point approach. Overall, 34 minima and 36 transition states have been characterized. Although we cannot prove the completeness of our conformation search, which proceeded without a rigorous protocol, we are confident that we have not missed low energy structures that may play important role in the processes we plan to study.

All calculations were performed using the Gaussian98[21] set of programs. All energies are relative to an arbitrarily chosen origin, species **1tt** (see Figure 1 for the structure and later text for notation). The geometry optimizations and frequency calculations were performed at the density functional theory level using B3LYP[22] energy functional with the 6-31G(d)[23] basis set. The relative energy at the B3LYP/6-31G(d) level is called E_1. To support the appropriateness of this basic level of calculations, single point energy calculations at the B3LYP/6-31G(d) optimized geometries were performed with the 6-31++G-

(18) (a) Christianson, D. W.; Lipscomb, W. N. *J. Am. Chem. Soc.* **1985**, *107*, 2682. (b) Mealli, C.; Sabat, M.; Marzilli, L. G. *J. Am. Chem. Soc.* **1987**, *109*, 1593. (c) Zhu, L.; Kostic, N. M. *Inorg. Chem.* **1987**, *26*, 4194. (d) Hansen, L. M.; Kumar, P. N. V. P.; Marynick, D. S. *Inorg. Chem.* **1994**, *33*, 728. (e) Hansen, L. M.; Derecskei-Kovacs, A.; Marynick, D. S. *J. Mol. Struct.* **1998**, *431*, 53. (f) Andruniow, T.; Zgierski, M. Z.; Kozlowski, P. M. *Chem. Phys. Lett.* **2000**, *331*, 509. (g) Andruniow, T.; Zgierski, M. Z.; Kozlowski, P. M. *J. Phys. Chem. B* **2000**, *104*, 10921. (h) Andruniow, T.; Zgierski, M. Z.; Kozlowski, P. M. *J. Am. Chem. Soc.* **2001**, *123*, 2679. (i) Kozlowski, P. M. *Curr. Opin. Chem. Biol.* **2001**, *5*, 736. (j) Andruniow, T.; Zgierski, M. Z.; Kozlowski, P. M. *J. Phys. Chem. A* **2002**, *106*, 1365. (k) Doelker, N.; Maseras, F.; Lledos, A. *J. Phys. Chem. B* **2001**, *105*, 7564.
(19) (a) Torrent, M.; Musaev, D. G.; Morokuma, K.; Ke, S.-C.; Warncke, K. *J. Phys. Chem. B* **1999**, *103*, 8618. (b) Ke, S.-C.; Torrent, M.; Musaev, D. G.; Morokuma, K.; Warncke, K. *Biochemistry* **1999**, *38*, 12681.
(20) (a) Golding, B. T.; Radom, L. *J. Chem. Soc., Chem. Commun.* **1973**, 939. (b) Golding, B. T.; Radom, L. *J. Am. Chem. Soc.* **1976**, *98*, 6331. (c) Golding, B. T. In *B_{12}*; Dolphin, D., Ed.; Wiley: New York, 1982; Vol. 1, pp 543−582. (d) Smith, D. M.; Nicolaides, A.; Golding, B. T.; Radom, L. *J. Am. Chem. Soc.* **1998**, *120*, 10223. (e) Smith, D. M.; Golding, B. T.; Radom, L. *J. Am. Chem. Soc.* **1999**, *121*, 1037. (f) Smith, D. M.; Golding, B. T.; Radom, L. *J. Am. Chem. Soc.* **1999**, *121*, 1383. (g) Smith, D. M.; Golding, B. T.; Radom, L. *J. Am. Chem. Soc.* **1999**, *121*, 5700. (h) Smith, D. M.; Golding, B. T.; Radom, L. *J. Am. Chem. Soc.* **1999**, *121*, 9388. (i) Smith, D. M.; Golding, B. T.; Radom, L. *J. Am. Chem. Soc.* **2001**, *123*, 1664. (j) Wetmore, S. D.; Smith, D. M.; Golding, B. T.; Radom, L. *J. Am. Chem. Soc.* **2001**, *123*, 7963. (k) Wetmore, S. D.; Smith, D. M.; Radom, L. *J. Am. Chem. Soc.* **2001**, *123*, 8678. (l) Semialjac, M.; Schwarz, H. *J. Am. Chem. Soc.* **2002**, *124*, 8974.
(21) Frisch, M. J.; Trucks, G. W.; Schlegel, H. B.; Scuseria, G. E.; Robb, M. A.; Cheeseman, J. R.; Zakrzewski, V. G.; Montgomery, J. A., Jr.; Stratmann, R. E.; Burant, J. C.; Dapprich, S.; Millam, J. M.; Daniels, A. D.; Kudin, K. N.; Strain, M. C.; Farkas, O.; Tomasi, J.; Barone, V.; Cossi, M.; Cammi, R.; Mennucci, B.; Pomelli, C.; Adamo, C.; Clifford, S.; Ochterski, J.; Petersson, G. A.; Ayala, P. Y.; Cui, Q.; Morokuma, K.; Malick, D. K.; Rabuck, A. D.; Raghavachari, K.; Foresman, J. B.; Cioslowski, J.; Ortiz, J. V.; Baboul, A. G.; Stefanov, B. B.; Liu, G.; Liashenko, A.; Piskorz, P.; Komaromi, I.; Gomperts, R.; Martin, R. L.; Fox, D. J.; Keith, T.; Al-Laham, M. A.; Peng, C. Y.; Nanayakkara, A.; Gonzalez, C.; Challacombe, M.; Gill, P. M. W.; Johnson, B.; Chen, W.; Wong, M. W.; Andres, J. L.; Gonzalez, C.; Head-Gordon, M.; Replogle, E. S.; Pople, J. A. *Gaussian98*, revision A.7; Gaussian, Inc.: Pittsburgh, PA, 1998.
(22) (a) Becke, A. D. *Phys. Rev. A* **1988**, *38*, 3098. (b) Becke, A. D. *J. Chem. Phys.* **1993**, *98*, 5648. (c) Lee, C.; Yang, W.; Parr, R. G. *Phys. Rev. B* **1988**, *37*, 785. (d) Hertwig, R. H.; Koch, W. *Chem. Phys. Lett.* **1997**, *268*, 345.
(23) (a) Hehre, W. J.; Ditchfield, R.; Pople, J. A. *J. Chem. Phys.* **1972**, *56*, 2257. (b) Hariharan, P. C.; Pople, J. A. *Theor. Chim. Acta* **1973**, *28*, 213.

Scheme 3. Potential Energy Surface for Open Isomers and the Transition States Connecting Them[a]

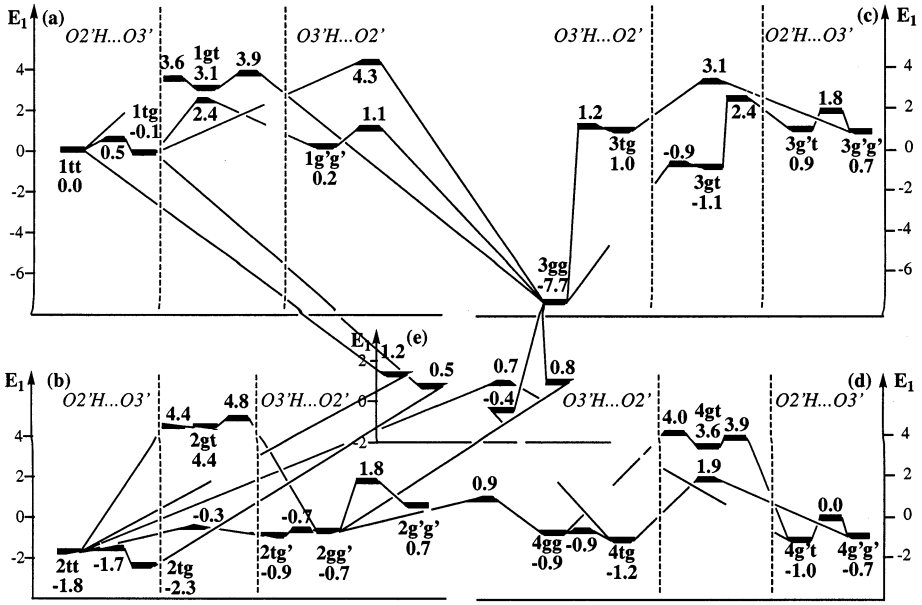

[a] The energy, E_1 (see section 2 for definition), is in kcal/mol. Parts a−d contain species **1**−**4**, respectively, and most TSs connecting them. Part e contains certain glycosyl rotation and pseudorotation TSs. In parts a−d, two modes of hydrogen bonding between 2′ and 3′ OH groups, O2′H···O3′ and O3′H···O2′, are distinguished (see also Table 2).

(d,p)[23,24] basis set using B3LYP (E_2), unrestricted (U)MP2(frozen core, FC)[25] (E_3), and projected unrestricted (PU)MP2(FC)[26] (E_4) methods. The B3LYP optimizations and single points were performed using the $10^{-5}/10^{-3}$ electrons criteria on convergence of the RMSD/maximum element of the density matrix difference between consequent SCF iterations. The B3LYP frequency calculations were performed using $10^{-6}/10^{-4}$ electrons thresholds. The SCF convergence criteria for MP2 calculations were the Gaussian default $10^{-8}/10^{-6}$ electrons.

The energies discussed in the text are E_1. All Hartree−Fock (HF−SCF) and Kohn−Sham (KS−SCF) calculations for our doublet species were spin unrestricted. The spin contamination in KS−SCF is negligible in all species, $\langle S^2 \rangle$ being less than 0.78. The HF−SCF spin contamination is also negligible for all open minima **1**−**4** (see later text for species notation), including the origin on the energy scale, and the transition states (TSs) connecting open minima ($\langle S^2 \rangle$ less than 0.77). Nevertheless, the HF−SCF determinant is substantially contaminated in (see later text for notation) **-C1** species ($\langle S^2 \rangle$ about 0.9), cyclic minima **5**−**6** ($\langle S^2 \rangle$ about 1.0), and cyclization TSs **TS-5**−**6** ($\langle S^2 \rangle$ about 1.1).

We find a reasonable agreement in the description of the sometimes problematic[27,28] hydrogen bonding energies between DFT and MP2. The E_2 (B3LYP/6-31++G(d,p)) values for open species agree with the nearly identical E_3 (UMP2/6-31++G(d,p)) and E_4 (PUMP2/6-31++G(d,p)) values to within 2 kcal/mol. The E_4 (PUMP2) values for spin-contaminated points agree with the E_2 (B3LYP) results to within 4 kcal/mol. Nevertheless, the E_3 (UMP2) values are higher than the E_4 (PUMP2) values by about 4 kcal/mol (**-C1** species), 10−11 kcal/mol (cyclic minima **5**−**6**), or even about 13 kcal/mol (cyclization TSs **TS-5**−**6**).

All the transition states structures and the reaction coordinates (Hessian eigenvectors with negative eigenvalues) were examined visually. Several less-trivial transition state structures, such as these involving ribose pseudorotation, were connected to the product on each side by using a small displacement from the TS along the reaction coordinate and a subsequent energy minimization.

3. Results and Discussion

Table 1 reports relative energies at four levels of calculation, as described in the previous section, and the selected geometrical parameters, shown in Scheme 1 and discussed later. The region of the PES corresponding to open minima (listed in Table 2) and the transition states interconnecting them is summarized in Scheme 3. The Cartesian coordinates of all species are collected in Supporting Information Table S1. Selected stationary points are depicted in Figure 1.

A. Open Conformations. Relative Ribose−Adenine Rotation. All located minima are classified as either open (four groups, **1**−**4**) or cyclic (5′,8-cycloadenosyl, groups **5** and **6**). The open 5′-deoxyadenosyl radical consists of two units, the rigid adenine and the flexible ribose. The relative orientation of the units is described by the glycosyl rotation angle, χ_{CN} (see Scheme 1 for angles definition). Commonly, the full range of glycosyl rotation angle values is divided into *anti* ($\chi_{CN} = 0° \pm 90°$) and *syn* ($\chi_{CN} = 180° \pm 90°$) regions.[29] All open minima reported in the present study are either *anti*, groups **1** and **3**, $\chi_{CN} = -30°$ to 70°, or on the *syn/anti* borderline, groups **2** and **4**, $\chi_{CN} = -110°$ to $-90°$. The located low energy glycosyl rotation transition states have $\chi_{CN} = -90°$ to $-45°$. In cyclic minima, the values of χ_{CN} fall into the ranges of 45°−55° in species **5** and 0°−20° in species **6**. The two groups of (tri) cyclic species differ in relative arrangements of ribose and adenine cycles: *exo*, as in species **5**, and *endo*, **6** (see Figure 1).

(24) Clark, T.; Chandrasekhar, J.; Spitznagel, G. W.; Schleyer, P. v. R. *J. Comput. Chem.* **1983**, *4*, 294.
(25) Head-Gordon, M.; Pople, J. A.; Frisch, M. J. *Chem. Phys. Lett.* **1988**, *153*, 503.
(26) (a) Schlegel, H. B. *J. Phys. Chem.* **1988**, *92*, 3075. (b) Schlegel, H. B. *J. Chem. Phys.* **1986**, *84*, 4530.
(27) (a) Csonka, G. I.; Anh, N.; Angyan, J.; Csizmadia, I. G. *Chem. Phys. Lett.* **1995**, *245*, 129. (b) Csonka, G. I.; Csizmadia, I. G. *Chem. Phys. Lett.* **1995**, *243*, 419. (c) Topol, I. A.; Burt, S. K.; Rashin, A. A. *Chem. Phys. Lett.* **1995**, *247*, 112. (d) Jeanvoine, Y.; Bohr, F.; Ruiz-Lopez, M. F. *Can. J. Chem.* **1995**, *73*, 710. (e) Florian, J.; Johnson, B. G. *J. Phys. Chem.* **1995**, *99*, 5899. (f) Novoa, J. J.; Sosa, C. *J. Phys. Chem.* **1995**, *99*, 15837. (g) Han, W.-G.; Suhai, S. *J. Phys. Chem.* **1996**, *100*, 3942. (h) Kang, H. C. *Chem. Phys. Lett.* **1996**, *254*, 135. (i) Jeong, H. Y.; Han, Y.-K. *Chem. Phys. Lett.* **1996**, *263*, 345. (j) Kang, H. C. *Chem. Phys. Lett.* **1996**, *263*, 348. (k) Zhang, Q.; Bell, R.; Truong, T. N. *J. Phys. Chem.* **1995**, *99*, 592.
(28) Callam, C. S.; Singer, S. J.; Lowary, T. L.; Hadad, C. M. *J. Am. Chem. Soc.* **2001**, *123*, 11743.
(29) Pullman, B.; Saran, A. *Prog. Nucleic Acid Res. Mol. Biol.* **1976**, *18*, 215.

Table 1. Relative Energies and Selected Structural Parameters for All Located Minima and Transition States

	relative energies[a]				structural parameters[b]					
species	E_1	E_2	E_3	E_4	χ_{CN}	ϕ_2	ϕ_3	P	θ_m	other
					open minima					
1tg	−0.1	0.2	0.0	0.0	−8.1	−144.7	88.3	7.5	36.7	O2′H···O3′, 2.11
1tt	0.0	0.0	0.0	0.0	−2.8	−154.7	−177.2	14.4	38.9	O2′H···O3′, 2.16
1tt-A1	0.2	0.2	−0.1	−0.1	−7.1	−153.5	−173.4	8.9	38.2	O2′H···O3′, 2.15
1gt	3.1	2.5	3.0	3.0	3.6	77.8	174.1	25.3	40.6	
1g′g′	0.2	1.1	0.9	0.9	−22.2	−36.4	−27.7	338.5	37.8	O3′H···O2′, 2.12; O2′H···O1′, 2.56
1g′g′-A1	0.8	1.4	2.0	2.0	25.7	−33.1	−28.7	355.1	35.5	O3′H···O2′, 2.12
1g′g′-A2	0.4	1.5	0.5	0.5	−28.8	−37.7	−24.4	320.5	39.9	O3′H···O2′, 2.07
2tg	−2.3	−2.4	−2.0	−2.0	−101.9	−140.8	95.8	30.9	35.7	O2′H···O3′, 2.02
2tt	−1.8	−2.3	−1.7	−1.7	−104.0	−150.4	174.1	33.4	37.7	O2′H···O3′, 2.07
2gt	4.4	3.2	4.2	4.2	−96.8	87.2	165.6	33.8	40.0	
2gg′	−0.7	−1.3	−0.2	−0.2	−94.8	101.6	−32.5	40.7	37.3	O3′H···O2′, 2.05
2tg′	−0.9	−1.3	−0.3	−0.3	−100.0	163.2	−50.6	48.3	35.5	O3′H···O2′, 2.25; O2′H···O3′, 2.68
2g′g′	0.7	1.0	2.0	2.0	−97.6	−45.0	−20.1	34.0	36.2	O3′H···O2′, 2.08
3g′t	0.9	0.3	1.5	1.5	50.4	−78.0	168.0	152.0	39.9	O2′H···O3′, 2.12
3g′g′	0.7	1.1	1.5	1.6	70.2	−87.3	−78.5	211.9	40.1	O2′H···O3′, 2.10; O3′H···O1′, 2.51
3g′g′-A1	1.9	3.1	2.0	2.0	−27.5	−95.8	−75.9	232.6	44.5	O2′H···O3′, 1.99
3gt	−1.1	−0.4	0.3	0.3	−20.9	62.7	172.6	183.2	40.0	O2′H···N3, 1.92
3gg	−7.7	−6.4	−5.7	−5.7	−16.6	57.8	37.4	167.9	37.6	O3′H···O2′, 2.07; O2′H···N3, 1.90
3tg	1.0	0.9	1.5	1.5	49.5	154.6	33.6	168.6	36.9	O3′H···O2′, 2.09
4g′t	−1.0	−1.2	−1.4	−1.4	−108.3	−81.7	169.4	181.5	36.4	O2′H···O3′, 2.09
4g′g′	−0.7	−0.1	−0.3	−0.3	−103.8	−86.6	−81.7	196.1	38.0	O2′H···O3′, 2.10; O3′H···O1′, 2.63
4gt	3.6	2.8	2.7	2.6	−106.0	82.5	180.0	177.6	41.1	
4gg	−0.9	−1.2	−1.4	−1.4	−104.6	80.4	46.2	172.8	38.2	O3′H···O2′, 2.16
4tg	−1.2	−1.3	−1.6	−1.6	−105.1	152.8	35.6	176.9	36.8	O3′H···O2′, 2.10
					open TSs					
TS-1gt-1tt	3.6	2.7	2.9	2.9	−7.2	116.5	173.6	13.6	40.6	O2′H···O3′, 3.29
TS-1tg-3gg	4.3	2.9	3.4	3.4	−12.3	126.8	77.1	8.6	39.3	O3′H···O2′, 3.23; O2′H···N3, 4.00
TS-1gt-3gg	3.9	3.2	3.3	3.3	3.1	74.5	124.9	25.6	38.9	O3′H···O2′, 3.57
TS-1g′g′-3gg	1.1	1.4	1.8	1.8	−7.5	5.0	−36.6	0.4	35.9	O3′H···O2′, 2.11; O2′H···N3, 4.31
TS-1tg-1g′g′	2.4	3.2	3.1	3.1	−34.2	−70.0	39.2	314.4	34.3	O2′H···O3′, 2.47; O3′H···O2′, 2.42
TS-1tg-1tt	0.5	0.2	0.1	0.1	−9.2	−156.3	135.3	9.3	36.6	O2′H···O3′, 2.15
TS-2gt-2gg′	4.8	3.4	4.3	4.3	−96.1	81.0	128.6	31.9	38.6	O3′H···O2′, 3.56
TS-2gt-2tt	4.4	3.1	4.1	4.1	−96.0	98.9	165.5	34.9	40.1	O2′H···O3′, 3.42
TS-2gg′-2tg′	−0.7	−1.4	−0.5	−0.5	−95.2	120.0	−33.7	45.3	37.4	O3′H···O2′, 2.06; O2′H···O3′, 3.20
TS-2gg′-2g′g′	1.8	1.5	2.8	2.9	−97.7	6.7	−33.9	35.7	36.2	O3′H···O2′, 2.05
TS-2tt-2tg	−1.7	−2.4	−2.3	−2.3	−103.5	−152.1	142.6	34.1	36.5	O2′H···O3′, 2.07
TS-2tt-2tg′	−0.3	−0.3	0.2	0.2	−105.0	−153.9	−109.4	36.1	34.7	O2′H···O3′, 2.09
TS-3gg-3tg	1.2	0.7	1.3	1.4	47.3	120.0	42.1	165.4	36.5	O3′H···O2′, 2.12; O2′H···N3, 4.29
TS-3g′t-3g′g′	1.8	1.7	2.5	2.5	59.5	−75.2	−124.5	182.6	37.2	O2′H···O3′, 2.15
TS-3tg-3g′g′	3.1	3.4	4.7	4.7	69.1	−158.7	−43.5	225.4	32.6	O2′H···O3′, 2.43; O3′H···O2′, 2.42
TS-3gt-3g′t	2.4	2.6	3.2	3.1	21.2	−28.7	175.9	160.5	43.2	O2′H···O3′, 2.78; O2′H···N3, 2.58
TS-3gg-3gt	−0.9	−0.5	0.3	0.3	−21.0	63.1	150.0	183.3	39.8	O3′H···O2′, 3.45; O2′H···N3, 1.92
TS-4gt-4g′t	3.9	2.9	2.7	2.7	−105.5	120.0	−177.0	178.7	40.5	O2′H···O3′, 3.60
TS-4gg-4gt	4.0	2.9	2.8	2.8	−105.7	81.8	141.3	176.5	41.2	O3′H···O2′, 3.37
TS-4gg-4tg	−0.9	−1.4	−1.9	−1.9	−105.1	120.0	44.2	174.3	36.7	O3′H···O2′, 2.14
TS-4tg-4g′g′	1.9	2.0	2.7	2.7	−104.2	−153.0	−43.9	194.1	28.3	O2′H···O3′, 2.43; O3′H···O2′, 2.48
TS-4g′t-4g′g′	0.0	0.1	−0.2	−0.2	−107.4	−77.7	−130.0	187.0	36.9	O2′H···O3′, 2.10
					glycosyl rotation					
TS-1tt-2tt	1.2	1.2	1.5	1.5	−46.9	−154.3	178.6	2.8	37.4	O2′H···O3′, 2.16
TS-1tg-2tg	0.5	0.9	0.8	0.8	−46.3	−142.3	87.3	353.5	36.2	O2′H···O3′, 2.10
TS-2gg′-3gg	0.8	0.6	1.3	1.3	−57.1	100.3	−35.7	8.0	34.8	O3′H···O2′, 2.10; O2′H···N3, 4.39
TS-3gg-4tg	−0.4	−1.3	−0.9	−0.9	−86.2	111.3	45.6	152.5	40.4	O3′H···O2′, 2.16; O2′H···N3, 3.33
					ribose pseudorotation					
TS-2tt-4g′t	0.7	0.0	1.8	1.8	−105.4	−79.1	91.0	116.8	36.4	O2′H···O3′, 2.10
TS-2gg′-4gg	0.9	−0.1	1.8	1.8	−97.4	146.0	3.5	107.8	39.6	O3′H···O2′, 1.94
					5′,8 cyclic minima					
5g′t	−16.4	−15.2	−1.3	−12.1	53.2	−101.6	−158.1	273.0	49.5	O2′H···O3′, 1.89
5tg′	−18.7	−16.4	−1.9	−12.7	55.0	−137.7	−67.8	265.2	50.7	O2′H···O3′, 2.03; O3′H···O1′, 2.65; C5′−C8, 1.55
5g′g	−19.3	−16.9	−2.2	−13.3	48.5	−41.0	4.6	282.9	51.8	O3′H···O2′, 1.95; O2′H···O1′, 2.44; C5′−C8, 1.55
5gg′	−17.0	−15.8	−1.5	−12.5	50.3	62.3	−21.0	275.4	49.5	O3′H···O2′, 1.92; C5′−C8, 1.55
6g′t	−12.7	−11.2	2.5	−7.9	11.1	−100.4	−171.1	273.1	48.5	O2′H···O3′, 1.89; C5′−C8, 1.55
6g′g′	−15.0	−12.4	1.0	−9.6	20.6	−116.5	−71.9	255.1	51.4	O2′H···O3′, 1.94; O3′H···O1′, 2.46; C5′−C8, 1.54
6g′g′-B1	−16.0	−13.4	−0.5	−10.9	4.3	−39.1	−5.3	289.6	51.3	O3′H···O2′, 1.96; O2′H···O1′, 2.38; C5′−C8, 1.55
6tg′	−14.7	−13.3	0.0	−10.3	7.0	139.3	−22.7	279.5	48.2	O3′H···O2′, 1.93; C5′−C8, 1.55
					5′,8 cyclization TSs					
TS-5g′t	11.6	12.0	26.9	13.9	70.9	−103.3	−157.3	271.8	44.1	O2′H···O3′, 1.88
TS-5tg′	9.5	11.0	26.0	13.0	71.9	−138.8	−69.0	263.8	45.3	O2′H···O3′, 2.02; O3′H···O1′, 2.74; C5′−C8, 2.27
TS-5g′g	9.4	10.9	26.2	13.0	67.5	−45.2	15.1	281.4	46.1	O3′H···O2′, 1.99; O2′H···O1′, 2.59; C5′−C8, 2.28
TS-5gg′	11.3	11.7	27.3	14.0	67.2	69.9	−20.5	277.7	43.9	O3′H···O2′, 1.91; C5′−C8, 2.28
TS-6g′t	13.4	14.2	28.4	15.2	−7.5	−125.6	178.9	289.5	44.7	O2′H···O3′, 1.92; C5′−C8, 2.21
TS-6g′g′	11.6	13.5	27.7	14.7	6.5	−108.9	−73.2	248.6	49.5	O2′H···O3′, 1.94; O3′H···O1′, 2.42; C5′−C8, 2.21
TS-6g′g′-B1	10.1	12.1	25.6	12.4	−10.1	−38.9	−13.7	296.8	48.2	O3′H···O2′, 1.99; O2′H···O1′, 2.34; C5′−C8, 2.22
TS-6tg′	11.3	12.2	26.1	13.2	−7.4	137.8	−27.7	285.7	44.3	O3′H···O2′, 1.96; C5′−C8, 2.21

Table 1. (Continued)

species	relative energies[a] E_1	E_2	E_3	E_4	structural parameters[b] χ_{CN}	ϕ_2	ϕ_3	P	θ_m	other
					8→5′ H transfer minima					
2tg-C1	9.6	11.0	18.1	13.8	−104.0	−138.2	92.2	30.5	34.6	O2′H···O3, 2.01
3gg-C1	5.8	8.3	15.2	11.4	−17.6	58.6	37.5	162.5	37.2	O3′H···O2, 2.06; O2′H···N3, 1.92

[a] Relative to species **1tt**, in kcal/mol. See section 2 for definitions of E_1 to E_4. [b] Dihedral angles in degree, distances in Å. See Scheme 1 and section 3 for definitions of structural parameters. For all species, all H···X (X = O1′, O2′, O3′, N3; see Scheme 1 for notation) distances of less than 3 Å are given. For open TSs, larger values of distances corresponding to forming/breaking hydrogen bonds are also given.

Table 2. Hydrogen Bonding between 2′-OH and 3′-OH Groups in the Located Open Minima[a]

Glycosyl conformation	Ribose conformation					
	3'-endo			2'-endo		
anti	b)	**1gt**	b)	**3gg**	**3gt**	b)
	1tg	**1tt**	b)	**3tg**	b)	b)
	b)	b)	**1g'g'**	b)	**3g't**	**3g'g'**
syn/*anti*	b)	**2gt**	**2gg'**	**4gg**	**4gt**	b)
	2tg	**2tt**	**2tg'**	**4tg**	b)	b)
	b)	b)	**2g'g'**	b)	**4g't**	**4g'g'**

[a] The four super cells, which differ in glycosyl orientation and ribose pucker of the enclosed species, are **1** (*anti*, 3′-*endo*), **2** (*syn*/*anti* borderline, 3′-endo), **3** (*anti*, 2′-*endo*), and **4** (*syn*/*anti* borderline, 2′-*endo*). Each super cell is a 3 by 3 matrix with value ranges, **g**, **t**, and **g′**, of ϕ_2 and ϕ_3 OH dihedrals defining, correspondingly, rows and columns. Borders denote the roles of the OH groups in the hydrogen bond between them: plain border, 2′-OH is the hydrogen donor; dashed border, 3′-OH is the donor. With the exception of species **2tg′**, the **t** and **g′** configurations of ϕ_2 (second and third rows of each supercell), as well as **g** and **g′** configurations of ϕ_3 (first and third columns of each supercell), are mutually exclusive because of hydrogen bonding between two OH groups. [b] No minimum has been located.

Ribose Ring Puckering. The five endocyclic ribose dihedrals, $\theta_0-\theta_4$, which characterize the ribose puckering, are described approximately using the pseudorotation phase, P, and amplitude, θ_m, as suggested by Altona and Sundaralingam:[30]

$$P = \arctan\left(\frac{\theta_2 + \theta_4 - \theta_1 - \theta_3}{2\theta_0(\sin 36° + \sin 72°)}\right) + X \qquad (1)$$

$$\theta_m = \theta_0/\cos P \qquad (2)$$

For $\theta_0 > 0$, $X = 0°$ if $\theta_2 + \theta_4 - \theta_1 - \theta_3 > 0$; otherwise, $X = 360°$. For $\theta_0 < 0$, $X = 180°$. The dihedral angles in the pseudorotational approximation are

$$\theta'_i = \theta_m \cos(P + i144°),\ i = 0-4 \qquad (3)$$

We find that this approximation works quite well; the absolute error, $|\theta'_i - \theta_i|$, which is larger for θ_1 and θ_4 than for three other dihedrals, does not exceed 2°. The full pseudorotation circle, $P = 0°-360°$, consists of two halves: northern, with $P = 0° \pm 90°$ corresponding to, most importantly, 3′-*endo* pucker (groups **1** and **2**) and southern, with $P = 180° \pm 90°$ and mainly 2′-*endo* ribose conformation, such as in species of groups **3** and **4**. The pseudorotation amplitude for the reported open minima falls within the 35°−42° range. The characteristic θ_0 (C1′−C2′−C3′−C4′) dihedrals for 3′-*endo* and 2′-*endo* configurations are correspondingly 25°−40° and −40° to −25°. The two located ribose puckering transition states have P values of 108° and 117°, corresponding to eastern pseudorotation barriers, in agreement with the previous studies[31] by Brameld et al. In cyclic minima, the ribose ring is more puckered, the amplitude θ_m being 48°−52°, and is no longer flexible, adopting an O1′-*exo* conformation with P in the range of 265°−290°.

Ribose Hydroxyl Groups. The optimal orientations of 2′ and 3′ OH groups, which are described by C1′−C2′−O2′−O2′H and C2′−C3′−O3′−O3′H dihedrals, ϕ_2 and ϕ_3,[29] respectively (Scheme 1), are determined by two factors. The first determinant of the shape of the energy profiles along ϕ_2 and ϕ_3 is the three substituents of the sp^3 carbons C2′ and C3′, respectively. Our notation for the minima reflects the 3-fold nature of the potential imposed by the substituents on the carbon atoms. Each of the two OH dihedrals, ϕ_2 followed by ϕ_3, is described by a letter corresponding to the range for the value: **g** for 0°−120°, **t** for 120° to −120°, **g′** for −120° to 0°. For instance, as seen from Table 1, in species **1tg**, $\phi_2 = -144.7°$ (**t**) and $\phi_3 = 88.3°$ (**g**). The 3-fold barriers imposed by the C2′ and C3′ substituents are typically about 1 kcal/mol.[32] Second, the ϕ_2 and ϕ_3 rotational profiles are shaped and coupled by the hydrogen bonding between the two OH groups. The energetic effect of hydrogen bonding is substantial, at least 3 kcal/mol (see Table 1 and discussion of isomers **1gt**, **2gt**, and **4gt** later), which results in the disappearance of several of the nine minima expected from two independent 3-fold potentials (Table 2). Species **6g′g′** and **6g′g′-B1**, although having both ϕ_2 and ϕ_3 in the same ranges (see Table 1), coexist as local minima.

5′-Methylene Group. The 5′ CH_2 group in the open species is close to being planar, with the H−C5′−C4′−H dihedral in the range of 160°−180° (for most species, 170°−180°). The orientation of this group is coupled to the rest of the radical mostly via repulsion of its hydrogens with the hydrogen of C8. We did not explore in detail the isomerism introduced by the orientation of 5′ CH_2 group and expect the corresponding stationary points to differ in energy by no more than about 1 kcal/mol. For most of the studied species, one of the H−C5′−C4′−O1′ dihedrals falls into the wide range of −50° to 30°. For species **1tt**, **1g′g′**, and **3g′g′**, isomers with different orientation of 5′ CH_2 group, denoted **-A1** and **-A2**, are listed in Table 1.

N6 Amino Group. In all studied species, the C6−NH_2 group is pyramidalized, with the H−N_{C6}−C6−H dihedral angle of about 160°. We find that the two sections of PES with opposite directions of pyramidalization have very similar shapes, with the energy differences between the corresponding stationary

(30) Altona, C.; Sundaralingam, M. *J. Am. Chem. Soc.* **1972**, *94*, 8205.

(31) Brameld, K. A.; Goddard, W. A., III. *J. Am. Chem. Soc.* **1999**, *121*, 985.

(32) (a) Morokuma, K.; Umeyama, H. *Chem. Phys. Lett.* **1977**, *49*, 333. (b) Pophristic, V.; Goodman, L. *J. Phys. Chem. A* **2002**, *106*, 1642.

points of about 1 kcal/mol. In all species reported in the present paper, the NH_2 pyramidalization direction is the same, with both H−N_{C6}−C6−N1 dihedral angles positive, one being about 10°, the other about 170°.

Energetic Effects of Internal Degrees of Freedom in Open Conformation. We find that structural motifs with the largest influence on the shape of the PES region corresponding to open structures (see Scheme 3, Table 1) are two hydrogen bonds (HBs): 2′-OH···N3 and the HB between the 2′-OH and 3′-OH groups. The isomer with both HBs, **3gg**, is the lowest among all open species, with the energy of −7.7 kcal/mol. Species without any HB, **1gt**, **2gt**, and **4gt**, have energies higher than 3 kcal/mol. Finally, isomers with a single HB, either 2′-OH···N3 (**3gt**) or 2′-O···3′-O (all other species), have energies in the approximate range of −2 to +1 kcal/mol.

We find that the only energetically pronounced coupling between the flexible degrees of freedom of the 5′-deoxyadenosyl radical is due to the 2′-OH···N3 sugar−base interaction, which is optimal with *anti* glycosyl orientation, 2′-*endo* ribose conformation, and **g** conformation of the 2′-OH group. In configurations without the 2′-OH···N3 HB, the influence of the glycosyl rotation and ribose conformation on the energies of the stationary points is quite mild. The average relative energies of all minima within the four groups, excluding species **1gt** to **4gt** and **3gg**, are 0.0 (**1**), −1.0 (**2**), 0.8 (**3**), and −1.0 (**4**) kcal/mol. Thus, it may be concluded that, generally, (a) *syn/anti* borderline species, **2** and **4**, are preferred over *anti*, **1** and **3**, and (b) 3′-*endo* species, **1** and **2**, lie lower in energy than 2′-*endo*, **3** and **4**. The second lowest minimum, **2tg**, which is 3′-*endo*, *syn/anti* borderline, lies 4−5 kcal/mol higher than the lowest minimum, **3gg** (Table 1).

The transition states connecting the open minima arise from (a) rotation about C2′−O2′ and/or C3′−O3′ bonds (the reaction coordinates being the ϕ_2 and ϕ_3 angles; see the corresponding columns in Table 1), (b) glycosyl rotation (see the χ_{CN} column), (c) ribose pseudorotation (the reaction coordinate being the pseudorotation phase, *P*), or, sometimes, a combination of these processes. We intentionally did not study all possible transition states, yet all the located minima are connected, with the highest TS lying at about +5 kcal/mol. On the pathway connecting all minima with at least one HB, the highest TS lies at +2.4 kcal/mol (see Scheme 3).

B. Intra-$AdCH_2^•$ C5′ Radical Reactions. The C5′ radical center may attack the adenine ring at the C8 atom, producing cyclic minima **5** and **6**. Because of the rigidity of the tricyclic skeleton, the number of cyclic isomers is substantially smaller. As seen from Table 1, cyclic minima **5** and **6** differ only in the values of the ϕ_2 and ϕ_3 dihedrals and lie substantially lower in energy than any open species, with **5** (−19 to −16 kcal/mol) being more stable than **6** (−16 to −13 kcal/mol). However, the cyclization barriers are relatively large. The lowest cyclization TS corresponds to formation of species **5g′g** and lies as high as 9.4 kcal/mol.

The hydrogen atom abstraction from C8 by the radical C5′ center is another process suggested[17] to take place in $AdCH_2^•$. Two of the isomers of the product of 8→5′ hydrogen transfer, species **2tg-C1** and **3gg-C1**, are structurally very similar to the corresponding $AdCH_2^•$ minima (see Table 1) yet lie more than 10 kcal/mol higher in energy. We did not study this endothermic hydrogen abstraction process in further detail.

C. Large Amplitude C5′ Movement via Relative Ribose−Adenine Rotation. We describe the large-amplitude motion of C5′ center, supposedly relevant to certain enzymatic processes involving coenzyme B_{12}, by performing a relaxed scan along one of the many possible coordinates called ROT, which is the C5′−C1′−N9−C4 dihedral angle (see Scheme 1 for atom notation). For each value of ROT (multiples of 15°), the rest of the radical was allowed to relax, minimizing the energy. Two configurations, 3′-*endo* **tt** and 2′-*endo* **gg**, were propagated along ROT. The results of the two scans are summarized in Figure 2, with Supporting Information Tables S2 and S3 providing further details. As expected from a one-dimensional scan, jumps in certain geometrical parameters are found. For example, the optimal χ_{CN} value undergoes a discontinuous change between ROT of −75° and −60° (Figure 2b; see also Tables S2 and S3).

Two features of the relaxed scans deserve attention. First, the potential energy well on the 2′-*endo* **gg** curve around the **3gg** minimum, determined by the attractive 2′-OH···N3 interaction (Figure 2e), besides being deep (about 5 kcal/mol), is quite extended along the glycosyl rotation coordinate (ROT range 75°−180°, χ_{CN} range −50° to 0°). Second, both 2′-*endo* **gg** and 3′-*endo* **tt** configurations with ROT of about −100° to −30° (χ_{CN} of about 70° to −150°) are substantially, by about 5 kcal/mol, destabilized. We explain this destabilization with two repulsive interactions between hydrogens of C2′ and C8 (Figure 2c) and between lone pairs of O1′ and N3 (Figure 2d). The qualitative mapping of our findings on another representation of the glycosyl rotation coordinate, the χ_{CN} dihedral angle, is given in Scheme 4.

D. Implications for the Function of the 5′-Deoxyadenosyl Group in AdoCbl-Dependent Enzymes. Extension of our free $AdCH_2^•$ gas-phase computational results to the structure and energetics of $AdCH_2^•$ in the active site of AdoCbl-dependent enzymes neglects the interactions of $AdCH_2^•$ with the surrounding polypeptide, the cobalt atom, the β-face of the corrin ring of the cobalamin moiety, any water molecules within the active site, and the bound substrate/product species. Nevertheless, the gas-phase calculations reveal features of the internal conformational energetics of $AdCH_2^•$ that provide insight into the possible role of the 5′-deoxyadenosyl moiety in the AdoCbl-dependent enzyme function. The results also serve as a starting point for future experimental and theoretical studies of cobalt−carbon bond cleavage and radical migration.

5′,8-Cyclization. A danger in the use of the 5′-deoxyadenosyl moiety to transfer radical character in the enzymes is the intramolecular reaction to form the catalytically inactive cyclic form. The calculated stability of the 5′,8-cycloadenosyl radical structures relative to the open forms is consistent with the experimentally observed[13a−c] formation of 5′,8-cycloadenosine in high yield in solution AdoCbl homolysis reactions. The calculations provide a partial explanation for the absence of this reaction path in the AdoCbl-dependent enzymes; the energy barrier for cyclization is higher than the energy barriers for conformational readjustments associated with the glycosyl rotation. In the enzyme active site, the lower barrier glycosyl rotation is followed by the rapid hydrogen atom abstraction from the substrate, decreasing the lifetime of the $AdCH_2^•$ species, and thus further decreasing the probability of the higher barrier cyclization process.

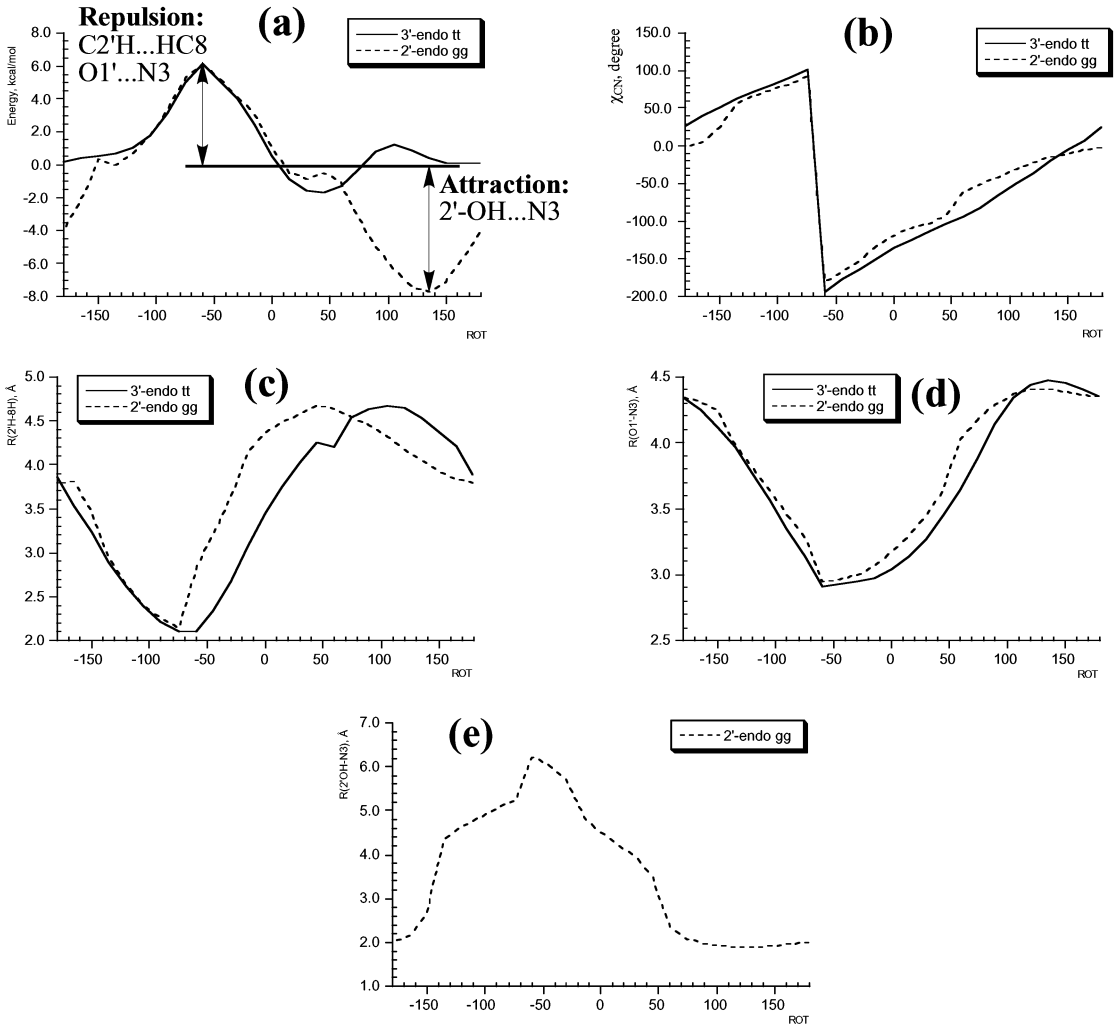

Figure 2. Results of the relaxed scans along the ROT coordinate, the C5′−C1′−N9−C4 dihedral angle: (a) energy; (b) χ_{CN} value; (c) distance between hydrogens of C2′ and C8; (d) distance between O1′ and N3; (e) distance between the hydrogen of 2′-OH and N3. Relative energy, E_1 (B3LYP/6-31G(d), relative to **1tt**, in kcal/mol), optimal geometrical parameters in degree (χ_{CN}) and Å (distances). Plain lines, 3′-*endo* **tt**; dashed lines, 2′-*endo* **gg**. The χ_{CN} values at ROT = −60°, 166.3° (3′-*endo* **tt**), and 179.6° (2′-*endo* **gg**) are depicted as the equivalent −193.7° and −180.4°.

Conformation of the 5′-Deoxyadenosyl Moiety in AdoCbl Crystals. The conformation of the 5′-deoxyadenosyl moiety in crystals[10] of coenzyme B_{12} is destabilized relative to the optimal conformations for the free $AdCH_2^•$ suggested by the present calculations. The strong 2′-OH···N3 hydrogen bond is absent, although two water molecules are situated suitably for formation of the 2′-OH···H_2O···H_2O···N3 hydrogen bonding chain. Moreover, the relative orientation of the ribose and adenine rings is characterized by $\chi_{CN} = 66.9°$ (ROT = −135°), a value close to the range of ribose−adenine repulsive interactions, as shown in Scheme 4 and Figure 2. Interactions other than the solely intra-$AdCH_2^•$ ribose−adenine 2′-OH···N3 attraction and 2′−H···H−C8 and O1′...N3 repulsions, such as the Co−C5′ bond, interactions with the corrin ring, and the hydrogen bonding chain involving water molecules, evidently stabilize the glycosyl orientation which is unfavorable for free $AdCH_2^•$.

Possible Roles of Ribose−Adenine Conformations and Energetics in Co−C Bond Activation and Homolysis. The X-ray crystallographic structures of AdoCbl-dependent enzymes have been determined under conditions, where atoms of the 5′-deoxyadenosyl moiety are missing or not well-resolved,[4,11b−e] with one exception. In the structure of a Class I (carbon skeleton rearranging) AdoCbl-dependent enzyme, glutamate mutase, Gruber et al.[12] identified two active site populations, distinguished particularly by the conformation of the 5′-deoxyadenosyl moiety. The so-called populations A and B differ in (a) the value of χ_{CN}, by 25° and (b) the ribose conformation, which is 2′-*endo* in A and 3′-*endo* in B. Population A was proposed to be a form of AdoCbl that is activated for Co−C cleavage, because of the remarkably long Co−C5′ distance of 3.1−3.2 Å. Population B was identified as a post-cleavage, post-substrate hydrogen atom abstraction state, where 5′-deoxyadenosyl is present as $AdCH_3$ (Co−C5′ distance of 4.5 Å). Pseudorotation of the ribose ring from 2′-*endo* to 3′-*endo* was proposed[12] as the primary coordinate for C5′ radical migration between cobalt and the substrate/product. The low internal barriers for ribose pseudorotation in the 5′-deoxyadenosyl moiety that we have calculated are in agreement with this proposal.

Comparison of the conformation of the 5′-deoxyadenosyl moiety in the "activated" coenzyme in population A of glutamate mutase with our calculated conformations strongly suggests that the 2′-OH···N3 hydrogen bond may exist in the 2′-*endo* form. Specifically, the 2′-*endo* conformation (species B in the protein database[33] entry 1I9C, $\chi_{CN} = 23.5°$, $P = 157.4°$, $\theta_m = 50.5°$, corresponding to population A discussed by Gruber et al.) has a 2′-O···N3 distance of only 3.03 Å. The 2′-O···N3 value in

Scheme 4. Structural Motifs Influencing the Free 5′-Deoxyadenosyl Energy Profile for the Relative Ribose−Adenine Rotation, Represented by the Glycosyl Dihedral Angle, χ_{CN}

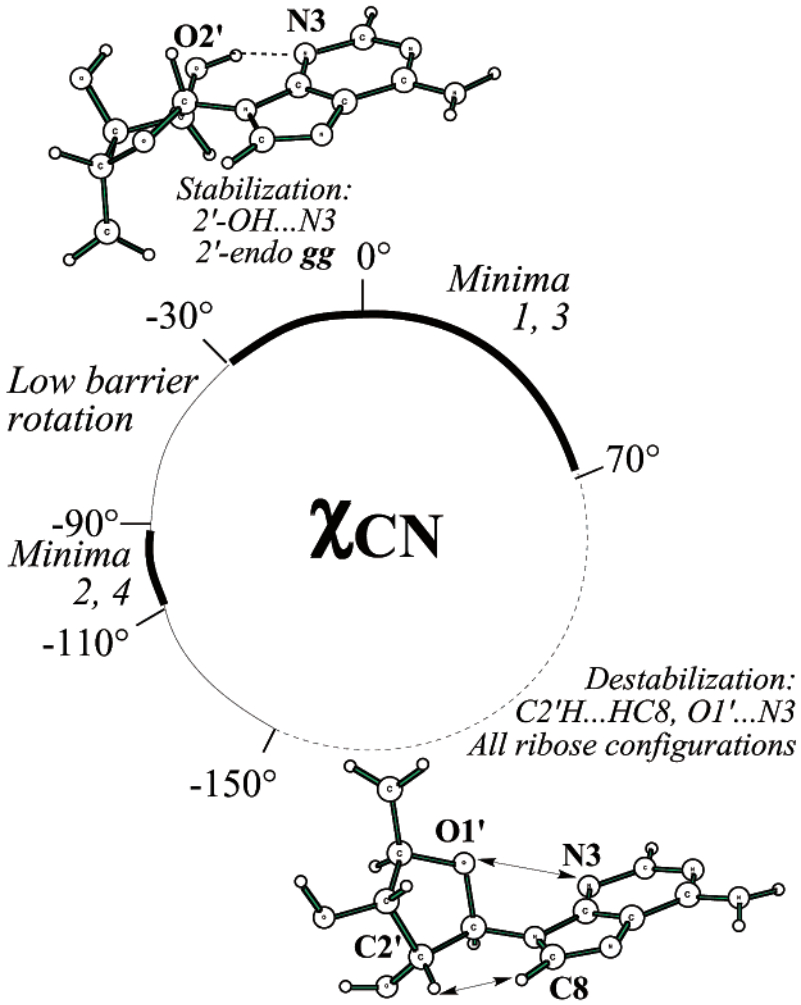

our minimum **3gg** ($\chi_{CN} = -16.6°$, $P = 167.9°$, $\theta_m = 37.6°$) is 2.82 Å. The 2′-OH···N3 hydrogen bonding motif in purine nucleosides has been studied both theoretically[29,34] and experimentally[35] in the 1970s but, to the best of our knowledge, has never been discussed within the context of coenzyme B_{12} structure or function. The presence of both the 2′-OH group and the N3 center, albeit as nearly every 5′-deoxyadenosyl heteroatom, was demonstrated[12,17,36] to be important for the functioning of the AdoCbl-dependent enzymes. Our computational results demonstrate that the change in the internal energy of $AdCH_2^•$ owing to the relative ribose−adenine rotation (see Scheme 4) is (a) within 4 kcal/mol in the χ_{CN} range of −110° to 70° for most ribose conformations, except for 2′-*endo* **gg**, for which it is about 8−10 kcal/mol, owing to the attractive 2′-OH···N3 interaction, and (b) within 8 kcal/mol for χ_{CN} = 70° to −110°, the determinants being the repulsive 2′−H···H−C8 and O1′···N3 interactions.

When these computational results are related to the experimentally determined conformations of the 5′-deoxyadenosyl moiety in solvated AdoCbl (assumed to be represented by AdoCbl crystals), $\chi_{CN} = 66.9°$, and in the population A species of Gruber et al.,[12] $\chi_{CN} = 23.5°$, it appears that the long-range attractive 2′-OH···N3 and, possibly, the repulsive 2′-H···H−C8 and O1′···N3 interactions contribute favorably to the formation of the AdoCbl population A within the enzyme. Thus, we suggest that the protein uses contributions from relaxation along the glycosyl rotation coordinate to labilize the Co−C bond in glutamate mutase. Protein-guided relaxation of the relative ribose−adenine rotational strain within the 5′-deoxadenosyl moiety might be a general mechanism that contributes to Co−C bond labilization, as illustrated in Scheme 5. The concept of protein involvement in the labilization of the Co−C bond through interactions with ribose and adenine was originally introduced by Pratt.[16]

Glycosyl Rotation as the Coordinate for Long-Range Radical Migration. The C5′-mediated radical migration in the Class I adenosylcobalamin-dependent mutases appears to be relatively short range (approximately ≤3 Å). In contrast, it has

(33) Berman, H. M.; Westbrook, J.; Feng, Z.; Gilliland, G.; Bhat, T. N.; Weissig, H.; Shindyalov, I. N.; Bourne, P. E. *Nucleic Acids Res.* **2000**, *28*, 235.
(34) Pullman, B.; Berthod, H. *Jerusalem Symp. Quantum Chem. Biochem.* **1973**, *5*, 209.
(35) (a) Witzel, H. *Prog. Nucleic Acid Res.* **1963**, *2*, 221. (b) Ts'o, P. O. P.; Rapaport, S. A.; Bollum, F. J. *Biochemistry* **1966**, *5*, 4153. (c) Broom, A. D.; Schweizer, M. P.; Ts'o, P. O. P. *J. Am. Chem. Soc.* **1967**, *89*, 3612. (d) Pitha, J. *Biochemistry* **1970**, *9*, 3678. (e) Ts'o, P. O. P. Monomeric Units of Nucleic Acids − Bases, Nucleosides, and Nucleotides. In *Fine Structure of Proteins and Nucleic Acids*; Fasman, G. D.; Timasheff, S. N. Eds.; Marcel Dekker: New York, 1970; p 49.
(36) (a) Zagalak, B.; Pawelkiewicz, J. *Acta Biochim. Pol.* **1965**, *12*, 219. (b) Toraya, T.; Ushio, K.; Fukui, S.; Hogenkamp, H. P. C. *J. Biol. Chem.* **1977**, *252*, 963. (c) Ichikawa, M.; Toraya, T. *Biochim. Biophys. Acta* **1988**, *952*, 191. (d) Calafat, A. M.; Taoka, S.; Puckett, J. M., Jr.; Semerad, C.; Yan, H.; Luo, L.; Chen, H.; Banerjee, R.; Marzilli, L. G. *Biochemistry* **1995**, *34*, 14125.

Scheme 5. Result of Coupling between the Co−C5′ Bond Scission and the 5′-Deoxyadenosyl Glycosyl Rotation for Two Hypothetical Limiting Cases[a]

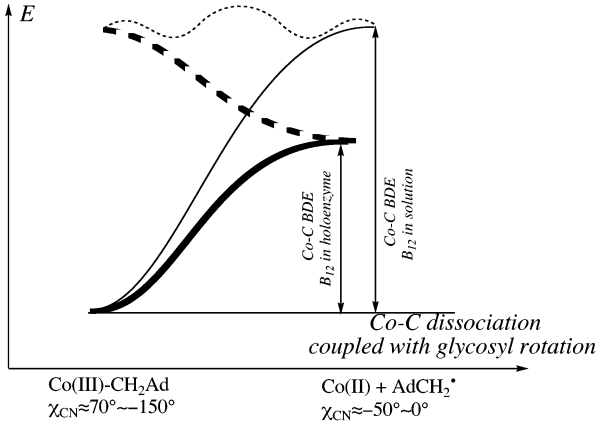

[a] Thick lines, within a holoenzyme; thin lines, in solution. Dashed lines, the $AdCH_2^•$ glycosyl rotation internal energy; plain lines, the energy profile of the coupled Co−C scission and glycosyl rotation. Within the holoenzyme, the shape of the glycosyl rotational profile is assumed to be determined mostly by the attractive 2′-OH···N3 and the repulsive 2′-H···H−C8 and O1′···N3 ribose−adenine interactions within $AdCH_2^•$. In solution, the energetic effect of intra-$AdCH_2^•$ ribose−adenine interactions is assumed to be largely diminished by hydrogen bonding with the solvent, as discussed in the text for the crystal structure of coenzyme B_{12}. The synergic coupling of the Co−C bond scission and the glycosyl rotation in the holoenzyme may be accomplished by restraints on both the Co−corrin[14b] and adenine[14b,15] moieties, as discussed by Masuda et al.[14b]

been shown that the C5′ radical migrates over 6−7 Å in the Class II eliminase enzyme, ethanolamine deaminase.[5] This long-range migration requires additional displacement of C5′ beyond that attainable through pseudorotation of the ribose ring. Pett et al. suggested, on the basis of computer graphics analysis, that C5′ displacements of up to 8 Å could be achieved by rotation about the ribose−adenine bond,[14a] and this motion has been incorporated explicitly in a molecular mechanism for the Class II diol dehydrase.[14b] The ROT energy profile presented in Figure 2 shows that the internal energetics of $AdCH_2^•$ are not inconsistent with a catalytically competent rotation on time scales less than $1/k_{cat}$, which sets an upper limit on the radical migration lifetime (typically, $k_{cat} \leq 10^2\ s^{-1}$ at $T \approx 298$ K for B_{12} enzymes,[1b] corresponding to Arrhenius activation energy barriers, $E_a \geq 15$ kcal/mol). Our DFT studies thus provide the first quantitative support for ribose−adenine rotation as a principal coordinate for long-range radical migration in coenzyme B_{12}-dependent enzymes.

4. Conclusions

The structural motifs determining the stability of the open isomers of 5′-deoxyadenosyl in gas phase are the hydrogen bonds between (i) 2′-OH and 3′-OH ribose groups and (ii) the 2′-OH ribose group and N3 atom of adenine. The most stable species, **3gg**, in which both hydrogen bonds exist lies at −7 to −6 kcal/mol on our energy scale; the second lowest isomer has the energy of about −2 kcal/mol. The energetic effects of the ribose puckering and the relative ribose−adenine orientation (glycosyl rotation) are smaller than those of the hydrogen bonding motifs.

All open species with at least one hydrogen bond are relatively easily interconvertible, the highest transition state lying at 2−3 kcal/mol. Ribose pseudorotation, rotations about C2′−O2′ and C3′−O3′ bonds, and rotation about the glycosyl bond inside the *anti* half-circle are all low-barrier processes.

The 5′,8-cyclization process, although strongly exothermic (by 10−20 kcal/mol) has relatively high barriers, with the lowest transition state lying at about 10 kcal/mol.

The eastern part (χ_{CN} of 70° to −150°) of the *syn* glycosyl rotation half-circle is substantially, by about 5−7 kcal/mol, destabilized by the repulsive 2′-H···H−C8 and O1′···N3 interactions.

The relative ribose−adenine rotation about the glycosyl bond may be associated with changes in the potential energy of 5′-deoxyadenosyl as large as 10−15 kcal/mol, depending on the ribose fragment conformation and the range of the rotation. Responsible for the energy change are the 2′-H···H−C8 and O1′···N3 repulsive and the 2′-OH···N3 stabilizing ribose−adenine interactions. The role of the potential energy associated with ribose−adenine interactions along the glycosyl rotation coordinate in the functioning of 5′-deoxyadenosyl-dependent enzymes deserves further attention. Hypothetically, the Co−C bond cleavage process in certain coenzyme B_{12}-dependent enzymes may be facilitated by coupling with the glycosyl rotation in a particular range. The coupling of Co−C bond scission and the relative ribose−adenine rotation may be accomplished via binding of the adenine ring and the Co−corrin fragment by the apoenzyme. The recent experimental structural findings of Gruber et al.[12] indirectly support the present hypothesis. Our DFT studies thus support the ribose−adenine rotation as a principal coordinate for long-range radical migration in coenzyme B_{12}-dependent enzymes.

Acknowledgment. We thank Profs. David Lynn and Luigi G. Marzilli for valuable discussions and Mr. Ilja V. Khavrutskii for technical assistance. The authors acknowledge grants from the National Science Foundation (CHE-9627775 to K.M.) and the National Institutes of Health (DK54514 to K.W.) and the generous support of computing time from NCSA. Acknowledgment is made to the Cherry L. Emerson Center of Emory University for the use of its resources, which is in part supported by a National Science Foundation grant (CHE-0079627) and an IBM Shared University Research Award.

Supporting Information Available: Cartesian coordinates of all optimized stationary points (Table S1) and relative energies and selected geometrical parameters of the relaxed scan points along ROT coordinate corresponding to 3′-*endo* **tt** (Table S2) and 2′-*endo* **gg** (Table S3) configurations. This material is available free of charge via the Internet at http://pubs.acs.org.

JA028393K